Available online at www.sciencedirect.com
ScienceDirect
Journal of Sound and Vibration 301 (2007) 106–125
JOURNAL OF SOUND AND VIBRATION
www.elsevier.com/locate/jsvi

Optimal passive control of adjacent structures interconnected with nonlinear hysteretic devices

M. Basili*, M. De Angelis

Department of Structural and Geotechnical Engineering, University of Rome, 'La Sapienza', Via Eudossiana 18, 00184 Rome, Italy

Received 1 August 2005; received in revised form 15 June 2006; accepted 12 September 2006
Available online 22 November 2006

Abstract

In this paper, the optimal passive control of adjacent structures interconnected by nonlinear hysteretic devices is studied. For nonlinear devices the versatile Bouc–Wen model is adopted, whereas for seismic excitation a Gaussian zero mean white noise and a filtered white noise are used. To solve nonlinear equations of motion a simplified solution is carried out using a stochastic linearization technique. The problem of the optimal design of the devices is studied and solved in the case of a simple two-degrees-of-freedom model. In the optimization problem, an energy criterion associated with the concept of optimal performance of the hysteretic connection is used. The energy performance index is defined as a measure of the ratio between the energy dissipated in the device and the seismic input energy on the structure. Only two parameters are considered in the optimization problem of the device yielding force and elastic stiffness. The rigid and elastic plastic models for the device are studied and compared. The design procedure leads to very simple indications on the optimal values of the device's mechanical parameters; these optimal values substantially depend only on the mass and stiffness ratio between the two structures. Finally, some concise results about the effectiveness of the hysteretic connection for the seismic response mitigation of coupled structures are also given.

1. Introduction

The control of structural vibrations can be done by using innovative techniques, such as passive, hybrid, semi-active and active control [1]. In civil engineering, the most useful technologies to provide seismic protection of structures are based on the passive control that can be provided through (i) base isolation, (ii) energy dissipation, and (iii) tuned mass dampers. Among these different passive control technologies, the one based on energy dissipation deserves special attention. This technique is based on the artificial increase of the dissipative capacity of the structural system through special dissipating devices. In order to obtain the most desiderable energy dissipation, the devices have to be placed in proper locations where relative motion between components is expected. Among the different situations in which energy dissipating devices can be beneficial [2], use of dissipative connections between either adjacent structures or adjacent parts of the same structure has received special attention [3–6]. A typical example is the one of contiguous buildings, which are usually

*Corresponding author. Tel.: +39 6 44585399; fax: +39 6 488 4852.
E-mail address: michela.basili@uniroma1.it (M. Basili).

0022-460X/$ - see front matter © 2006 Elsevier Ltd. All rights reserved.
doi:10.1016/j.jsv.2006.09.027

separated by structural joints and connected through of dissipative devices. Another example is the dissipative coupling of wall and frame, where the wall acts as stiffening element. In both situations, it is essential that the two structures have different dynamic properties, so that relative movements may develop during their dynamic response.

The concept of dissipative connection between adjacent structures has found several application in Japan, [7–10]. Dissipative connections have also been proven beneficial in preventing pounding damage between adjacent buildings [11].

Typically, passive energy dissipation devices are modelled as linear elements, e.g. viscoelastic [1,12] and fluid viscous dampers [1,13], or nonlinear hysteretic elements, e.g. steel elastic plastic [1,14–16] and friction dampers [1,17–18].

In a large part of the available literature referring to adjacent structures coupled with passive dampers, the dampers are modelled as linear elements, with constant viscous damping and, in some cases, also constant stiffness arranged in parallel and series [19–22]. The principal aim of these works is to provide indications about the optimal design of the dissipative connection using different design principles and using both two and multi dof adjacent systems. Only few works are present in the literature that involve nonlinear devices with an elastic or rigid plastic behavior, sometimes referred to as hysteretic dampers. Typically, these studies are about coupled structures modelled as multi dof systems. As an example, the work of Ni et al. [23–24] show a parametric study of two adjacent multi dof systems, having 20 and 10 floors, respectively, in order to evaluate the optimal parameters of hysteretic connections and their optimal positions and numbers.

Among the very few works which give simple, concise and general information about optimal design of hysteretic devices, the work by De Angelis and Ciampi [3] has to be cited, where a rational design criterion for the hysteretic connection is proposed.

This study aims to present a simple approach to the optimal design of hysteretic dampers connecting two adjacent structures, each modelled as a single dof system, and excited by ground motion. In order to describe the nonlinear behavior of the damper the Bouc–Wen model is adopted and only two parameters, (the yield force and elastic stiffness), are considered in the optimization procedure. The optimum parameters of the hysteretic damper are determined by an energy criterion [2]. The optimal design of both a rigid plastic device, RPD, defined by one parameter, the yield force, and an elastic plastic device, EPD, defined by two parameters, the elastic stiffness and the yield force, is considered. The results for both devices are compared, leading to useful information for the optimal design. The seismic analysis is developed by a stochastic approach, and a simplified solution of the nonlinear problem is carried out by stochastic linearization [25,26]. In order to obtain brief results a white noise, WN, ground excitation is used first. Then, the optimal design procedure is extended by using a more realistic filtered white noise, FWN, ground excitation.

2. Coupled structure systems

2.1. Structural model

The most basic representation of the coupled structures problem is the two-degrees-of freedom system (2-dofs) as shown in Fig. 1. The two structures, each modelled as an elastic one-dof, are connected with a dissipative coupling link. This simple model is used for investigating the effectiveness of using dissipative passive devices as connections between two structures, to reduce dynamic response of each structural system. Such case is then compared to the case in which the structures are rigidly connected and the case in which they are completely independent, as proposed in [3].

The equations of motion for such a system, excited by a base acceleration, $\ddot{y}_g(t)$, are:

$$\begin{cases} m_1\ddot{y}_1 + c_1\dot{y}_1 + k_1 y_1 = F(t) - m_1\ddot{y}_g(t), \\ m_2\ddot{y}_2 + c_2\dot{y}_2 + k_2 y_2 = -F(t) - m_2\ddot{y}_g(t), \end{cases} \tag{1}$$

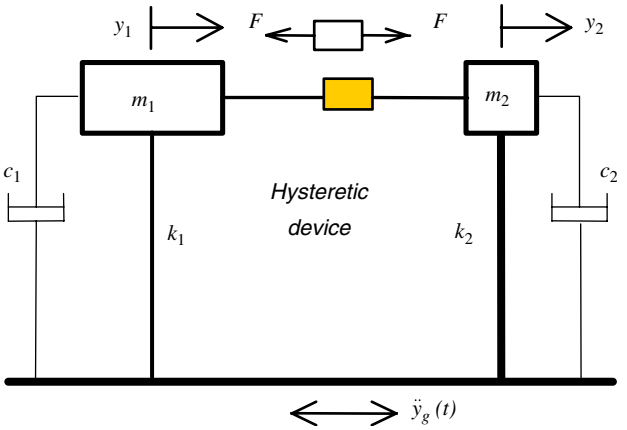

Fig. 1. The structural model.

where m_i, k_i and c_i $(i = 1, 2)$ are the mass, stiffness and damping coefficient, respectively, y_i $(i = 1, 2)$, are the relative displacements, while $F(t)$ is the force in the connection. Introducing the following parameters:

m_1: mass of the first structure
$T_1 = 2\pi/\omega_1 = 2\pi(m_1/k_1)^{1/2}$: natural period of the first structure
$\xi_i = c_i/2m_i\omega_i$ $(i = 1, 2)$: damping ratio (both assumed 5%)
$\lambda = k_2/k_1$: stiffness ratio
$\mu = m_2/m_1$: mass ratio
$\tilde{F}(t) = F(t)/m_1$: normalized force in the passive device connection

the structural model is completely described by:

$$\begin{cases} \ddot{y}_1 + 2\xi_1\omega_1\dot{y}_1 + \omega_1^2 y_1 = \tilde{F}(t) - \ddot{y}_g(t), \\ \ddot{y}_2 + 2\xi_2\omega_2\dot{y}_2 + \omega_2^2 y_2 = \dfrac{\tilde{F}(t)}{\mu} - \ddot{y}_g(t), \end{cases} \tag{2}$$

where $\omega_2^2 = \omega_1^2\lambda/\mu$.

2.2. The hysteretic devices

Let us assume that two adjacent structures shown in Fig. 1 are interconnected by a nonlinear hysteretic damping device. These devices present a high capacity of hysteresis damping, through plastic deformation or friction, and are characterized by stable and non-degrading mechanical behavior.

The Bouc–Wen model [26] has been and still is commonly used in the field of structural engineering in many applications, especially in the random vibration field. This success is principally related to its versatility and especially to the possibility of expressing the linearization coefficients in a closed form, as will be discussed in the next paragraphs.

Using the Bouc–Wen model to represent hysteretic behavior, the restoring force has the following expression:

$$F(t) = C_1\Delta y + C_2 z, \tag{3}$$

with $\Delta y = y_2 - y_1$ and where:

$$C_1 = v\frac{F_y}{u_y}, \tag{4}$$

$$C_2 = (1 - v)F_y, \tag{5}$$

where v is the post-to-pre-yield stiffness ratio, F_y the yield force and u_y the yield displacement.

The function z is related to Δy through the following first-order nonlinear differential equation:

$$\dot{z} + g(z, \Delta\dot{y})\Delta\dot{y} = 0, \tag{6}$$

with:

$$g(z, \Delta\dot{y}) = \gamma \operatorname{sgn}(\Delta\dot{y}) z|z|^{n-1} + \beta|z|^n - A, \tag{7}$$

where A, β, γ and n are model parameters.

Usually, Eq. (7) is expressed in non-dimensional form as $\bar{g}(z, \Delta\dot{y}) = g(z, \Delta\dot{y})u_y$, with dimensionless parameters $\bar{A} = Au_y$, $\bar{\beta} = \beta u_y$, $\bar{\gamma} = \gamma u_y$ and n. Parameters $\bar{\beta}$ and $\bar{\gamma}$ control the shape of the hysteresis loop, $\bar{A}$ the restoring force amplitude, and n the smoothness of the transition from elastic to plastic response.

As shown in Fig. 2, if the parameters respect the conditions $\bar{\beta} + \bar{\gamma} = 1$ and $\bar{A} = 1$, F_y and u_y have the meaning of yield force and yield displacement, respectively.

The Bouc–Wen model is useful for its capability of reproducing different types of deformation paths; in fact, by properly selecting the model parameters, it can describe different constitutive laws, softening as well as hardening, with and without degradation.

Since typical experimental hysteresis loops, e.g. steel EPDs, Fig. 3, show small values of post-yield stiffness, the parameter v is fixed equal zero. Therefore, the restoring force can be expressed:

$$F(t) = C_2 z = F_y z, \tag{8}$$

$$\tilde{F}(t) = (F_y/m_1)z. \tag{9}$$

In general, the parameters describing the Bouc–Wen hysteretic model are $\bar{A}$, $\bar{\beta}$, $\bar{\gamma}$, n F_y, k_c, v. In design problems, some parameters can be fixed a priori, while others are the design variables. In this paper, the dimensionless model parameters of the connecting damper are assumed to be $\bar{A} = 1$, $\bar{\beta} = 0.5$, $\bar{\gamma} = 0.5$ and $n = 1$, $v = 0$, whereas F_y, yielding force, and $k_c = F_y/u_y$, elastic stiffness, are selected by using an optimal design criterion.

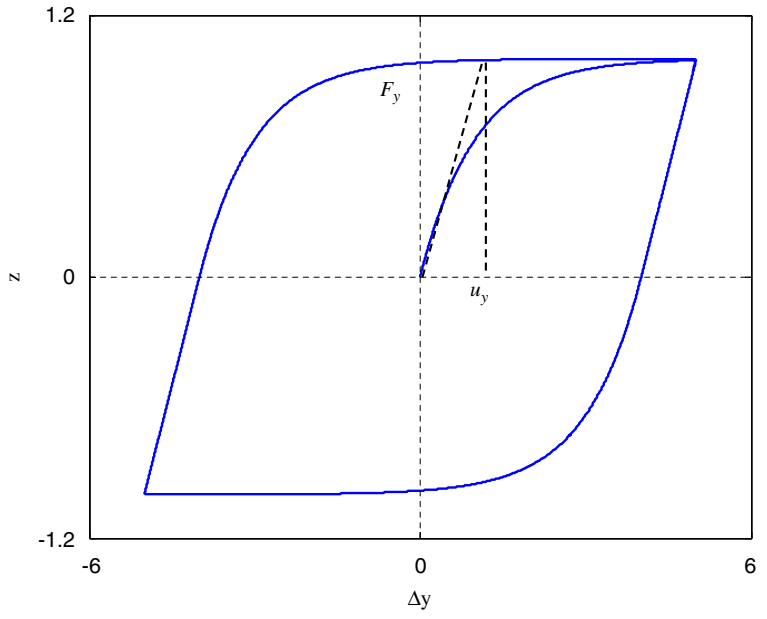

Fig. 2. $z(y)-\Delta y$ graph for $\bar{A} = 1$, $\bar{\beta} = 0.5$, $\bar{\gamma} = 0.5$, $n = 1$. F_y and u_y have the meaning of yield force and yield displacement.

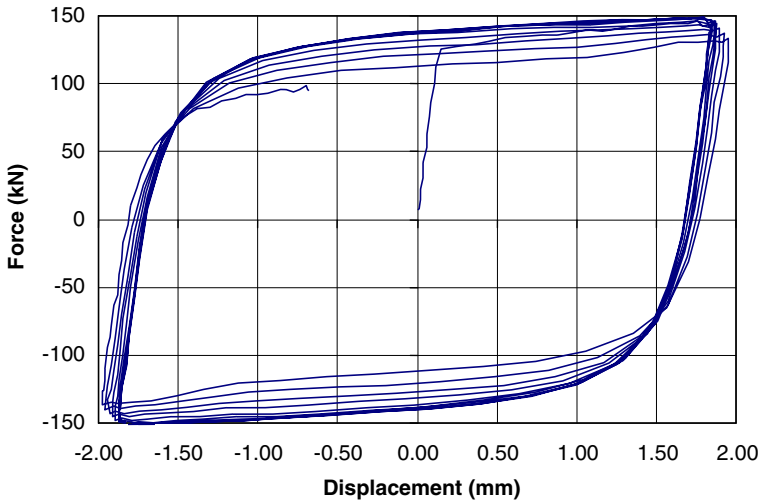

Fig. 3. Experimental force–displacement relation for a steel elastic plastic device.

2.3. Seismic excitation model

In the field of structural engineering more and more frequently probabilistic methodologies are used in order to asses, in a rational way, the structural safety. Especially in the field of structural dynamics, the excitations related to natural phenomena, such as seismic excitation, have an unquestionable probabilistic character.

In this study, a Gaussian zero mean white noise, WN, stochastic input, characterized by its power spectral density S_0 is first considered. Subsequently, the ground excitation is also modelled as a filtered white noise, FWN, corresponding to the Kanai–Tajimi spectrum [27–28]. The time domain equation of the Kanai–Tajimi filter is

$$\ddot{y}_g + 2\xi_g\omega_g\dot{y}_g + \omega_g^2 y_g = -\ddot{y}_{\mathrm{br}}, \tag{10}$$

where $\ddot{y}_{\mathrm{br}}$ is the excitation at the bedrock.

When approaching zero frequency, earthquakes have low energy contents. To better represent the real frequency content of seismic excitations at low frequencies, an additional filter is typically prepended to the Kanai–Tajimi filter [29].

In time domain analysis, the equations representing the two filters are

$$\begin{cases} \ddot{y}_g + 2\xi_g\omega_g\dot{y}_g + \omega_g^2 y_g = 2\xi_p\omega_p\dot{y}_p + \omega_p^2 y_p + \ddot{y}_{\mathrm{br}}(t), \\ \ddot{y}_p + 2\xi_p\omega_p\dot{y}_p + \omega_p^2 y_p = -\ddot{y}_{\mathrm{br}}(t). \end{cases} \tag{11}$$

Here, the bedrock excitation is considered a zero mean Gaussian WN process, $E[\ddot{y}_{\mathrm{br}}(t)] = 0$, where $E[\cdot]$ indicates the expected value, with autocorrelation $E[\ddot{y}_{\mathrm{br}}(s)\ddot{y}_{\mathrm{br}}(t)] = 2\pi\delta(s-t)$.

The parameters of the first filter are assumed as $\omega_g = 12\,\mathrm{rad/s}$ and $\xi_g = 0.6$ (Soong and Gregoriou [30]), whereas the second filter has $\omega_p = 2.2\,\mathrm{rad/s}$ and $\xi_p = 0.6$ (Clough and Penzien [29]). Fig. 4 shows the power spectral density of the two seismic excitation models. It is clear that the second model (11), shows a better representation of seismic excitation at low frequencies with respect to the first model (10).

2.4. Stochastic equivalent linearization

Since the connecting damper is a nonlinear hysteretic device, Eq. (2) are also nonlinear. Having considered a stochastic seismic excitation, it is possible to find a simplified solution of Eq. (2) by means of a stochastic linearization technique [23,25]. In fact, when the seismic excitation is a zero-mean stationary Gaussian process, the equations of motion are directly linearized in closed form, and the coefficients of the linearized system are

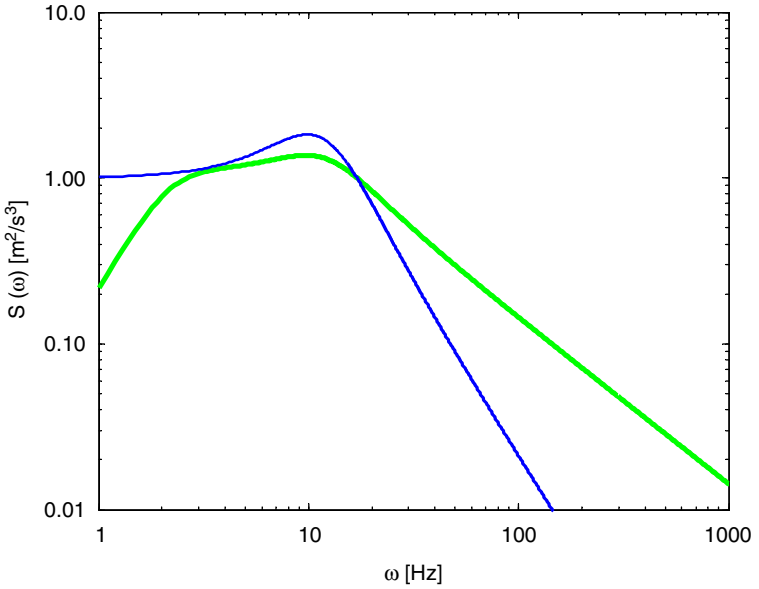

Fig. 4. Power spectral density of ground excitation. Kanai–Tajimi filter, double filter.

obtained as algebraic functions of the response variable statistics. In this case, Eq. (6), representing the hysteretic connecting device, has the following linearized equivalent form:

$$\dot{z} + C_e \Delta\dot{y} + K_e z = 0. \tag{12}$$

The two coefficients C_e and K_e can be evaluated in terms of the second moments of $\Delta\dot{y}$ and z, and, for $n = 1$, they have the following expressions [25]:

$$C_e = \sqrt{\frac{2}{\pi}}\left[\beta\sqrt{E[z^2]} + \gamma\,\frac{E[\Delta\dot{y}z]}{\sqrt{E[\Delta\dot{y}^2]}}\right] - A, \tag{13}$$

$$K_e = \sqrt{\frac{2}{\pi}}\left[\gamma\sqrt{E[\Delta\dot{y}^2]} + \beta\,\frac{E[\Delta\dot{y}z]}{\sqrt{E[z^2]}}\right], \tag{14}$$

where the terms $\sqrt{E[z^2]}$ and $\sqrt{E[\Delta\dot{y}^2]}$ are, respectively, the standard deviations of variables z and $\Delta\dot{y}$, while $E[\Delta\dot{y}z]$ is the covariance of the above mentioned variables.

2.5. Equation of motion in the space state

Having considered a stochastic input, the seismic excitation, the responses and the physical parameters of the hysteretic device can be normalized in the following way:

$$\ddot{\hat{y}}_{\mathrm{br}} = \frac{\ddot{y}_{\mathrm{br}}(t)}{\sqrt{2S_0\omega_1}}, \tag{15}$$

$$\hat{y}_i = \frac{y_i(t)}{\sqrt{2S_0\omega_1}} \quad \text{with } i = 1, 2, \tag{16}$$

$$\hat{F} = \frac{\tilde{F}}{\sqrt{2S_0\omega_1}} = \eta_y z, \tag{17}$$

$$\hat{\gamma} = \frac{\bar{\gamma}}{\eta_y}\,\gamma_c \lambda \omega_1^2, \tag{18}$$

$$\hat{\beta} = \frac{\bar{\beta}}{\eta_y}\,\gamma_c \lambda \omega_1^2, \tag{19}$$

$$\hat{A} = \frac{\bar{A}}{\eta_y}\,\gamma_c \lambda \omega_1^2, \tag{20}$$

with:

$$\eta_y = \frac{F_y}{m_1 \sqrt{2 S_0 \omega_1}}, \tag{21}$$

$$\gamma_c = k_c / k_2, \tag{22}$$

where η_y is the normalized yield force of the hysteretic device and γ_c the stiffness ratio.

Considering these new definitions, Eqs. (2), (9) and (12) can be rewritten in the space state, as a system of first-order differential equations:

$$\dot{\mathbf{X}}(t) = \mathbf{A}\mathbf{X}(t) + \mathbf{B}e(t), \tag{23}$$

in which:

$$\mathbf{X}(t) = \begin{bmatrix} \hat{y}_1 & \hat{y}_2 & z & \dot{\hat{y}}_1 & \dot{\hat{y}}_2 \end{bmatrix}^{\mathrm{T}}, \tag{24}$$

$$\mathbf{B} = \begin{bmatrix} 0 & 0 & 0 & 1 & 1 \end{bmatrix}^{\mathrm{T}}, \tag{25}$$

$$e(t) = -\ddot{\hat{y}}_g(t), \tag{26}$$

$$\mathbf{A} = \begin{bmatrix} 0 & 0 & 0 & 1 & 0 \\ 0 & 0 & 0 & 0 & 1 \\ 0 & 0 & -\hat{K}_e & \hat{C}_e & -\hat{C}_e \\ -\omega_1^2 & 0 & \eta_y & -2\xi_1\omega_1 & 0 \\ 0 & -\omega_2^2 & -\eta_y/\mu & 0 & -2\xi_2\omega_2 \end{bmatrix}, \tag{27}$$

where "T" indicates the transpose.

Expressions (24)–(27) are valid when seismic input is the WN. If seismic input is an FWN, described in Section 2.3, the expressions (24)–(27) change as follows:

$$\mathbf{X}(t) = \begin{bmatrix} \hat{y}_1 & \hat{y}_2 & z & \dot{\hat{y}}_1 & \dot{\hat{y}}_2 & \hat{y}_g & \dot{\hat{y}}_g & \hat{y}_p & \dot{\hat{y}}_p \end{bmatrix}^{\mathrm{T}}, \tag{28}$$

$$\mathbf{B} = \begin{bmatrix} 0 & 0 & 0 & 0 & 0 & 0 & -1 & 0 & 1 \end{bmatrix}^{\mathrm{T}}, \tag{29}$$

$$e(t) = -\ddot{\hat{y}}_{\mathrm{br}}(t), \tag{30}$$

$$\mathbf{A}=\begin{bmatrix} 0 & 0 & 0 & 1 & 0 & 0 & 0 & 0 & 0 \\ 0 & 0 & 0 & 0 & 1 & 0 & 0 & 0 & 0 \\ 0 & 0 & -\hat{K}_e & \hat{C}_e & -\hat{C}_e & 0 & 0 & 0 & 0 \\ -\omega_1^2 & 0 & \eta_y & -2\xi_1\omega_1 & 0 & \omega_g^2 & 2\xi_g\omega_g & 0 & 0 \\ 0 & -\omega_2^2 & -\eta_y/\mu & 0 & -2\xi_2\omega_2 & \omega_g^2 & 2\xi_g\omega_g & 0 & 0 \\ 0 & 0 & 0 & 0 & 0 & 0 & 1 & 0 & 0 \\ 0 & 0 & 0 & 0 & 0 & -\omega_g^2 & -2\xi_g\omega_g & \omega_p^2 & 2\xi_p\omega_p \\ 0 & 0 & 0 & 0 & 0 & 0 & 0 & 0 & 1 \\ 0 & 0 & 0 & 0 & 0 & 0 & 0 & -\omega_p^2 & -2\xi_p\omega_p \end{bmatrix}. \tag{31}$$

2.6. Solution of equations of motion

Defining with $\mathbf{G_{XX}} = E[\mathbf{X}\mathbf{X}^{\mathrm{T}}]$ the covariance matrix of $\mathbf{X}$, Lin has proved [31] that $\mathbf{G}_{\mathrm{XX}}$ satisfies the following differential equation:

$$\dot{\mathbf{G}}_{\mathbf{XX}} = \mathbf{A}\mathbf{G}_{\mathbf{XX}} + \mathbf{G}_{\mathbf{XX}}\mathbf{A}^{\mathrm{T}} + \frac{\pi}{\omega_1}\mathbf{B}\mathbf{B}^{\mathrm{T}}. \tag{32}$$

For the stationary response of the system under stationary random excitation, Eq. (32) reduces to the algebraic Liapunov equation:

$$\mathbf{A}\mathbf{G}_{\mathbf{XX}} + \mathbf{G}_{\mathbf{XX}}\mathbf{A}^{\mathrm{T}} + \frac{\pi}{\omega_1}\mathbf{B}\mathbf{B}^{\mathrm{T}} = \mathbf{0}. \tag{33}$$

It is important to note that matrix $\mathbf{A}$ depends on $\mathbf{G_{XX}}$, since $\hat{C}_e$ and $\hat{K}_e$ are related to response statistics. Then Eq. (33) is nonlinear and an iterative procedure is required to solve it. To start the iteration, at the first step, the solution of a linear system can be used, with a stiffness equal to the pre-yield stiffness, k_c, of the nonlinear device. Rearranging the covariance matrix of the response, $\mathbf{G_{XX}}$, in the vector $\mathbf{G}$, to reach a converged solution requires solving iteratively Eq. (33) until the quantity $\|\mathbf{G}^{k+1} - \mathbf{G}^{k}\|/\|\mathbf{G}^{k}\|$ is sufficiently small.

The statistics $E[\Delta\dot{y}^2]$, $E[\Delta\dot{y}z]$ and so on, can be obtained from the covariance matrix of the output vector $\mathbf{X}_e = \mathbf{C}\mathbf{X}$:

$$\mathbf{G}_{\mathbf{X}_e\mathbf{X}_e} = E[\mathbf{X}_e\mathbf{X}_e^{\mathrm{T}}] = \mathbf{C}\mathbf{G}_{\mathbf{XX}}\mathbf{C}^{\mathrm{T}}, \tag{34}$$

where $\mathbf{C}$ is the output matrix.

3. Energy approach as design criterion of the dissipative connection

In order to give an optimal design of the nonlinear dissipative hysteretic device, different criteria may be followed. The most useful criterion for seismic design refers to energy-based methods, [1]. Here, an energy criterion associated with the concept of optimal performance of the dissipative connection is used. The idea is that the connection performs at its best if it is capable of dissipating as much as possible of the energy input by the earthquake.

In order to consider the energy balance in our problem, let us start from Eq. (2) where the relative energy balance of the structural system is defined [32]:

$$E_k(t) + E_{\mathrm{dc}}(t) + E_e(t) = E_F(t) + E_i(t), \tag{35}$$

where:

$$E_k(t) = \frac{1}{2}(\dot{y}_1^2 + \mu\dot{y}_2^2), \tag{36}$$

is the *kinetic energy* of the system;

$$E_{\mathrm{dc}}(t) = \int_0^t 2\xi_1\omega_1\dot{y}_1^2\,\mathrm{d}t + \mu\int_0^t 2\xi_2\omega_2\dot{y}_2^2\,\mathrm{d}t, \tag{37}$$

is the *energy dissipated* by linear viscous damping in the structural system;

$$E_e(t) = \frac{1}{2}(\omega_1^2 y_1^2 + \mu\omega_2^2 y_2^2), \tag{38}$$

is the *elastic energy* of the system;

$$E_F(t) = E_{\mathrm{eF}} + E_{\mathrm{dF}}, \tag{39}$$

is the *energy associated* with the device, which can be considered the sum of an elastic term, E_{eF}, and of a dissipative term, E_{dF}.

Finally,

$$E_i(t) = -\int_0^t \ddot{y}_g\,\mathrm{d}y_1 - \mu\int_0^t \ddot{y}_g\,\mathrm{d}y_2, \tag{40}$$

is the relative input energy.

It is noteworthy that each term of the energy balance (Eqs. (36)–(40)) is normalized with respect to the mass, m_1, of the first structure.

To select the optimal device, an energy performance index, named EDI, energy dissipation index, is used. The index is defined as the ratio of the maximum value of the energy dissipated in the dissipation device, to the corresponding maximum value of the energy input by the earthquake, both evaluated over time:

$$\mathrm{EDI} = \frac{(E_{\mathrm{dF}})_{\mathrm{MAX}}}{(E_i)_{\mathrm{MAX}}}. \tag{41}$$

In [2], it is demonstrated that maximizing EDI leads to satisfactory design for a large class of applications of passive control.

In order to formulate the *relative energy balance* in the stochastic approach, Eq. (35) can be rewritten in terms of the mean values:

$$E[E_k] + E[E_{\mathrm{dc}}] + E[E_e] = E[E_F] + E[E_i], \tag{42}$$

where:

$$E[E_k] = \frac{1}{2}[E[\dot{\hat{y}}_1^2] + \mu E[\dot{\hat{y}}_2^2]], \tag{43}$$

$$E[E_{\mathrm{dc}}] = 2\left[\xi_1\omega_1 E[\dot{\hat{y}}_1^2] + \xi_2\omega_2\mu E[\dot{\hat{y}}_2^2]\right]t, \tag{44}$$

$$E[E_e] = \frac{1}{2}[\omega_1^2 E[\hat{y}_1^2] + \mu\omega_2^2 E[\hat{y}_2^2]. \tag{45}$$

To estimate the mean value of the energy associated to the connection, $E[E_F]$, it is convenient to assume that the force in the connection device has the following constitutive differential law (Eqs. (12) and (17)):

$$\dot{\hat{F}}(t) = -\eta_y\hat{C}_e\Delta\dot{\hat{y}} - \hat{K}_e\hat{F}(t). \tag{46}$$

A similar expression is obtained using a Maxwell model for the device. Such a model consists of a linear spring, k_M, and a linear viscous damper, c_M, in series:

$$\dot{F}(t) = k_M\Delta\dot{y} - \frac{k_M}{c_M}F(t). \tag{47}$$

Dissipated and elastic energies associated to the Maxwell device have the following form:

$$E[E_{\mathrm{dF}}] = \frac{E[F^2]}{c_M}\, t, \tag{48}$$

$$E[E_{\mathrm{eF}}] = \frac{E[F^2]}{k_M}, \tag{49}$$

where $E[F^2]$ represents the expected value of the restoring force of the device. Comparing the two expressions, (46) and (47), leads to:

$$c_M = -\eta_y \frac{\hat{C}_e}{\hat{K}_e} \quad \text{and} \quad k_M = -\eta_y \hat{C}_e, \tag{50}$$

and using Eqs. (48) and (49):

$$E[E_{\mathrm{dF}}] = -\hat{K}_e \frac{E[\hat{F}^2]}{\eta_y \hat{C}_e}\, t, \tag{51}$$

$$E[E_{\mathrm{eF}}] = -\frac{E[\hat{F}^2]}{\eta_y \hat{C}_e}. \tag{52}$$

Since $\hat{C}_e$ is negative, c_M, k_M, $E[E_{\mathrm{dF}}]$ and $E[E_{\mathrm{eF}}]$ are positive quantities.

This analysis shows that the equivalent linearization of a nonlinear hysteretic device identifies an equivalent viscoelastic Maxwell model.

Considering the energy increments corresponding to a time increment Δt, the energy balance (42) is rewritten as:

$$E[\Delta E_{\mathrm{dc}}] + E[\Delta E_{\mathrm{dF}}] = E[\Delta E_i], \tag{53}$$

or in explicit form:

$$2\left[\xi_1 \omega_1 E[\dot{\hat{y}}_1^2] + \xi_2 \omega_2 \mu E[\dot{\hat{y}}_2^2]\right]\Delta t + \hat{K}_e \frac{E[\hat{F}^2]}{\eta_y \hat{C}_e}\, \Delta t = E[\Delta E_i]. \tag{54}$$

In Eqs. (53) and (54), both the expected values of elastic and kinetic energies disappear because they do not depend on t.

At this point, a new definition of EDI index, used in the stochastic approach, can be derived considering a time interval Δt:

$$\mathrm{EDI} = \frac{E[\Delta E_{\mathrm{dF}}]}{E[\Delta E_i]} = \frac{E[\Delta E_{\mathrm{dF}}]}{E[\Delta E_{\mathrm{dc}}] + E[\Delta E_{\mathrm{dF}}]}. \tag{55}$$

In order to maximize EDI, it is necessary: (i) to reduce the energy input and/or (ii) to increase the dissipative capabilities by modifying the physical characteristics of the dissipative system.

In the passive control strategies, the capacity of dissipating energy is increased by using special devices expressly made for the purpose.

In the particular case of WN input, Inaudi et al. [33], demonstrated that for single dof system the expected value of the dissipated energy is:

$$E[E_{\mathrm{dc1}}] = \pi S_0 t. \tag{56}$$

Here, according with the normalization Eqs. (15)–(20), Eq. (56) becomes:

$$E[E_{\mathrm{dc1}}] = \frac{\pi}{2\omega_1}\, t. \tag{57}$$

Consequently, for an uncoupled 2dofs, the total energy dissipated by the system is:

$$E[E_{dc1}] + E[E_{dc2}] = \frac{\pi}{2\omega_1}(1+\mu)t. \tag{58}$$

In this study it has been numerically verified that the total dissipated energy is equal to:

$$E[E_{dc1}] + E[E_{dc2}] + E[E_{dF}] = \frac{\pi}{2\omega_1}(1+\mu)t. \tag{59}$$

Each term depends on the structural parameters. This consideration leads to the important result that the total dissipated energy is independent on the position and type of dissipative connection.

Consequently, Eq. (53), the increment of input energy has the following simple expression:

$$E[\Delta E_i] = \frac{\pi}{2\omega_1}(1+\mu)\Delta t, \tag{60}$$

which is particularly useful when performing an analysis with the WN process. In fact in this case, maximizing the EDI index is equivalent to maximizing the dissipated energy $E[\Delta E_{dF}]$. On the contrary, for the FWN process, the two quantities, mean value of ΔE_{dF} and EDI, are not equal.

Finally, it is important to note that Eq. (55) does not depend on the time increment Δt, and that the same expression of EDI in the stochastic approach can be obtained by writing the power balance.

4. Optimal design of the system with RPD and with white noise input

To evaluate the effectiveness of the solution, some response quantities will be considered, such as:

$$Y = \sqrt{E[(\hat{y}_i)^2]}/\sqrt{E[(\hat{y}_i^0)^2]} : \text{relative displacements } (i = 1, 2);$$

$$A_i = \sqrt{E[(\ddot{\hat{y}}_i)^2]}/\sqrt{E[(\ddot{\hat{y}}_i^0)^2]} : \text{absolute accelerations } (i = 1, 2);$$

$$\Delta Y = \sqrt{E[(\hat{y}_2 - \hat{y}_1)^2]}/\sqrt{E[(\hat{y}_2^0 - \hat{y}_1^0)^2]} : \text{relative displacements between the two structures.}$$

where $\hat{y}_i^0, \ddot{\hat{y}}_i^0$ are, respectively, displacements and absolute accelerations obtained for the uncoupled system.

The optimal passive control of adjacent structures excited by WN seismic input and connected by a rigid plastic device, RPD, has been studied. In this case, the hysteretic device is defined only by the normalized yield force η_y, whereas the two parameters λ, stiffness ratio, and μ, mass ratio, completely define the two structures.

For a given couple of values of the parameters λ and μ ($\mu = 1$, $\lambda = 5$), the stochastic response, as a function of η_y, has been evaluated, Fig. 5. The graph includes three typical situations: (i) no connection, $\eta_y \to 0$, (ii) dissipative connection, $0 < \eta_y < 10$, and (iii) rigid connection, $\eta_y > 10$. The two limit cases, no connection and rigid connection, respectively, are important for comparison purposes. The optimal yield force has been selected as the one which maximizes the EDI index value. Such a force also produces a general and simultaneous reduction of all response quantities. The effectiveness of the dissipative connection clearly results by the comparison with the cases of the uncoupled and rigidly connected structures, since all response quantities appear substantially reduced with respect to both cases. However, this is not always true, since there are also cases where, for different values of λ and μ, in particular when the mass of the second structure is comparatively smaller $\mu = 0.1$, an increment of Y_2 is observed, Fig. 6.

A concise presentation of the results of an extended parametric analysis is shown in Fig. 7, in which, for some values of λ, the optimal η_y values versus μ are reported.

By looking at Fig. 7, it appears that all curves present a discontinuity for $\mu = \lambda$. This is because when the two structures have the same vibration period, the connection cannot be activated. In any case, the optimal parameter of the dissipative rigid plastic connection has a very regular behavior. Moreover, it is possible to observe that for low μ, the optimal η_y value increases with λ while, for large μ, it decreases with λ. However, the preliminary design of an hysteretic connection may be performed with reference to an RPD and Fig. 7 provides a very simple way for optimal design of hysteretic connections in adjacent structures.

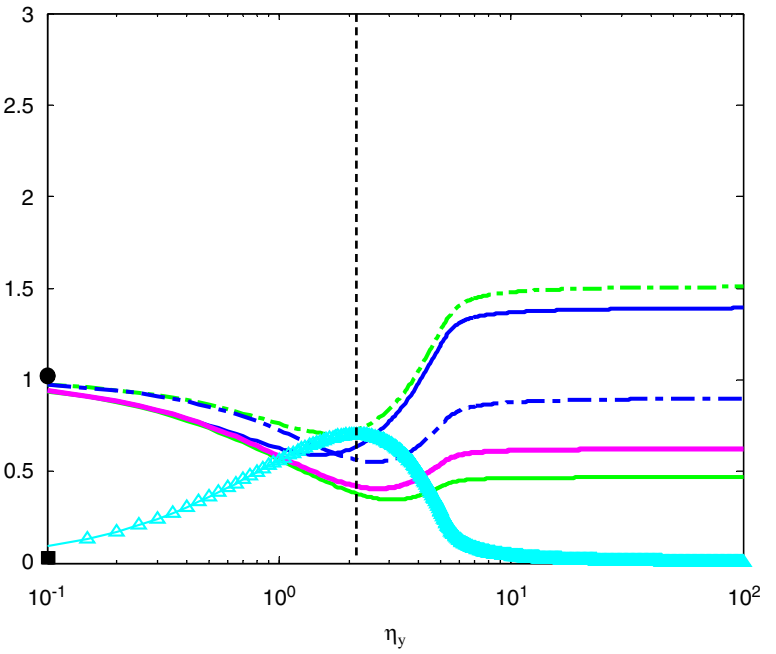

Fig. 5. WN and RPD: EDI index and response quantities versus η_y, $\mu = 1$, $\lambda = 5$. ● responses for $\eta_y = 0$. ■ EDI for $\eta_y = 0$. --- $\eta_{y,\mathrm{opt}}$. Y_1, Y_2, A_1, A_2, ΔY, EDI.

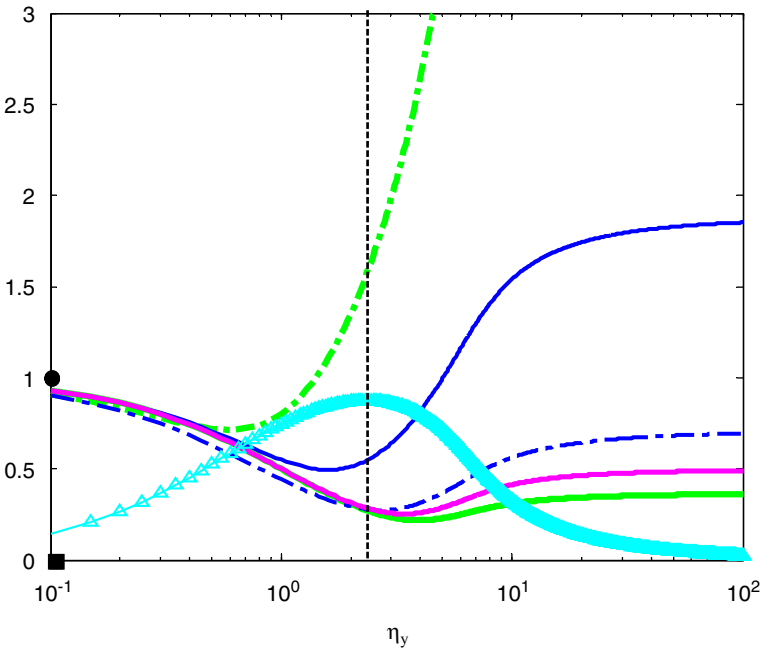

Fig. 6. WN and RPD: EDI index and response quantities versus η_y, $\mu = 0.1$, $\lambda = 5$. ● responses for $\eta_y = 0$. ■ EDI for $\eta_y = 0$. --- $\eta_{y,\mathrm{opt}}$. Y_1, Y_2, A_1, A_2, ΔY, EDI.

Moreover, it is possible to estimate the effectiveness of the connection in order to reduce the structural response of the system. In fact, the response reduction by using a RPD, designed by using the spectrum of Fig. 7 obtained under WN excitation, can be considered for different values of the structural parameters

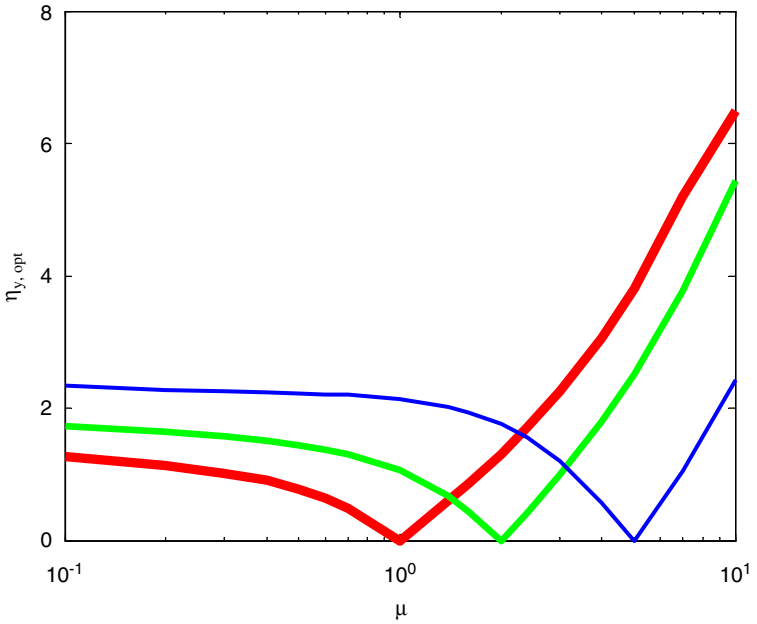

Fig. 7. WN and RPD: Optimal design spectrum: $\lambda = 1$, $\lambda = 2$, $\lambda = 5$.

μ and λ, Fig. 8. By looking at the single quantity, there are more regions where the seismic response is reduced with respect to no connection case. In particular, Fig. 8a shows that $\mu < \lambda$ is preferable for reducing the displacement of the first structure, Y_1; moreover, the reduction improves when the relative stiffness λ increases. The best reduction of the second structure in term of displacement, Y_2, instead, occurs when $\mu > \lambda$. The use of dissipative connections leads always to reduction of the absolute accelerations, A_1 and A_2, and the relative displacement, ΔY, as Figs. 8b and c, respectively, show.

Indeed, these results can be used in different applications regarding some typical control and design problems of adjacent structures. Different approaches may be considered with regard to (i) control strategies and (ii) design parameters.

For case (i), two control strategies may be considered:

- Global protection,
- Selective protection.

In global protection, the attention is focused on protecting both structures. In selective protection, it is important to reduce the vibration response of only one structure (here defined as structure 1, *main structure*), with possible sacrifice of the other structure, (here defined as structure 2, *auxiliary* or *secondary structure*).

For case (ii), two situations may occur:

- The first is the design of the entire system, where all quantities, λ, μ and η_y, are design parameters; for the WN input case, this situation coincides with the case in which the first structure is considered known;
- In the second situation, the two structures may pre-exist, and consequently λ, μ are considered known, while only the connection device is unknown. In this case the design problem is to determine the yield force of the hysteretic device.

It is clear that the two approaches presented here must be considered together. In fact, there could be the situation where the first structure exists, whereas the second structure and the connection have to be designed. In addition, it may be requested that the entire system be protected against earthquake damage. In this case, for example, the λ and μ values can be selected by the graphs of Fig. 8. If the goal is protecting both structures,

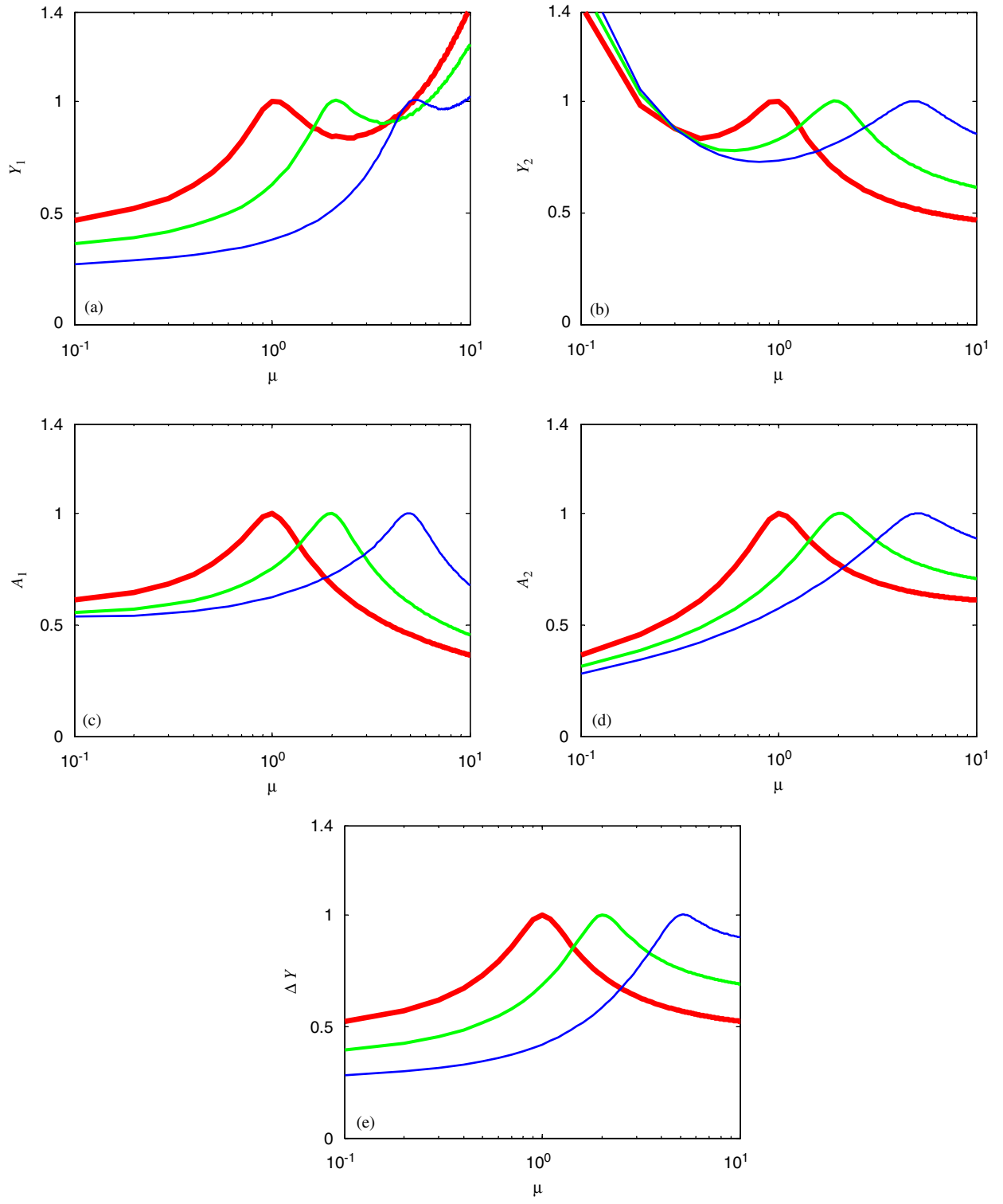

Fig. 8. WN and RPD: (a) and (b) Relative displacements of the first and the second structure versus μ and λ; (c) and (d) Absolute accelerations of the first and the second structure versus μ and λ; (e) relative displacements between the two structures versuss μ and λ. $\lambda = 1$, $\lambda = 2$, $\lambda = 5$.

a good choice of the structural parameters could be $\mu = 0.8$ and $\lambda = 5$. Using RPD leads to reduction of ~60% for Y_1, the displacement of the first structure, and ~30% for Y_2. Moreover, normalized accelerations A_1 and A_2 are reduced by over 40%. Corresponding to these values of λ and μ, the optimal yield force $\eta_y = 2.1$ of the hysteretic device is obtained by using the spectrum of Fig. 7.

Similarly, when the attention is focused on the main structure only (selective protection), λ could be chosen equal to 5, as the previous case, while μ could have small values (0.1–0.2). This situation can represent the case of structural control with dissipative bracing. The protected structure has a reduction of ~70% for the displacement, while the acceleration is reduced by over 40%. Finally, by using curves of Fig. 7, the selection of the optimal parameter for the hysteretic connection leads to $\eta_y = 2.2$.

5. Applications of the methodology to practical problems

The optimal design methodology defined in the last section, can be easily applied and extended to solve practical problems by using more realistic modelling, for both the device and the seismic input.

In fact, considering the difficulties of realizing a RPD, an elastic plastic device, EPD, should be considered. The EPD is characterized by two parameters, η_y and γ_c, Eqs. (21) and (22). In the RPD the parameter γ_c was omitted because it approaches infinity ($\gamma_c \to \infty$). As an example, for given values of λ and μ, Fig. 9 shows contour lines of the EDI index versus η_y and γ_c. An important observation can be immediately made: the EDI index does not show a well defined maximum versus γ_c. This means that, while it is possible to select an optimal value for the yield force, $\eta_y \approx 1.5$, the same is not possible for the relative stiffness γ_c. However, it results also that, for $\eta_y = 1.5$, $\gamma_c = 1$ already leads to a value of the index close to its maximum. This is also confirmed by Fig. 10, where, for the optimal value of η_y, the response quantities are presented as function of γ_c. For $\gamma_c \geqslant 1$ the EDI index does not practically increase, while at $\gamma_c = 1$ all the response quantities appear substantially reduced. This conclusion, which was already suggested in a previous work, De Angelis [3], allows us to design an EPD by fixing $\gamma_c = 1$, and by optimizing only η_y.

Fig. 11 presents the optimal design curves of the η_y parameter of an EPD with $\gamma_c = 1$ compared with corresponding curves obtained for an RPD. The two design spectra appear very close to each other expecially for high values of the stiffness ratio λ. From this observation, it emerges that the optimal design for an hysteretic connection is simply carried out by fixing $\gamma_c = 1$ and by using, for the optimal η_y parameter, the design spectrum of Fig. 7. For this reason, an EPD is adopted in the following applications.

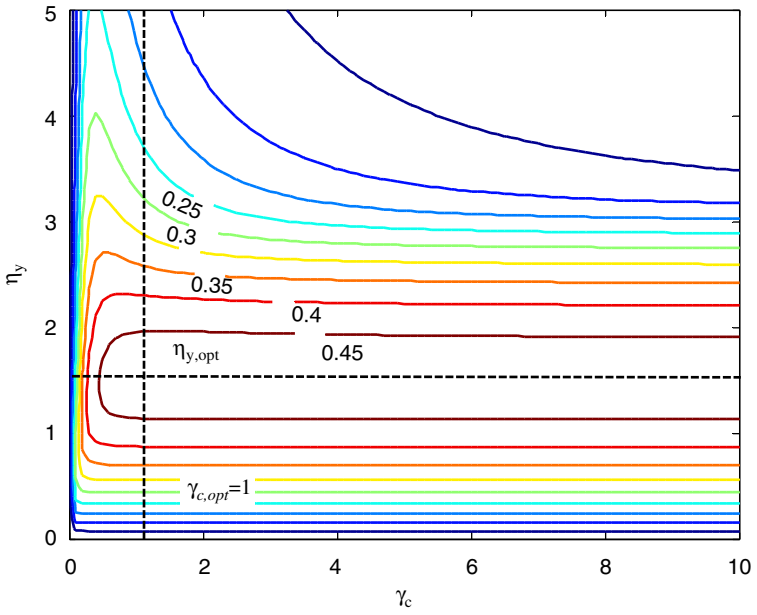

Fig. 9. WN and EPD: EDI contour lines versus η_y and γ_c, $\mu = 1$, $\lambda = 2$.

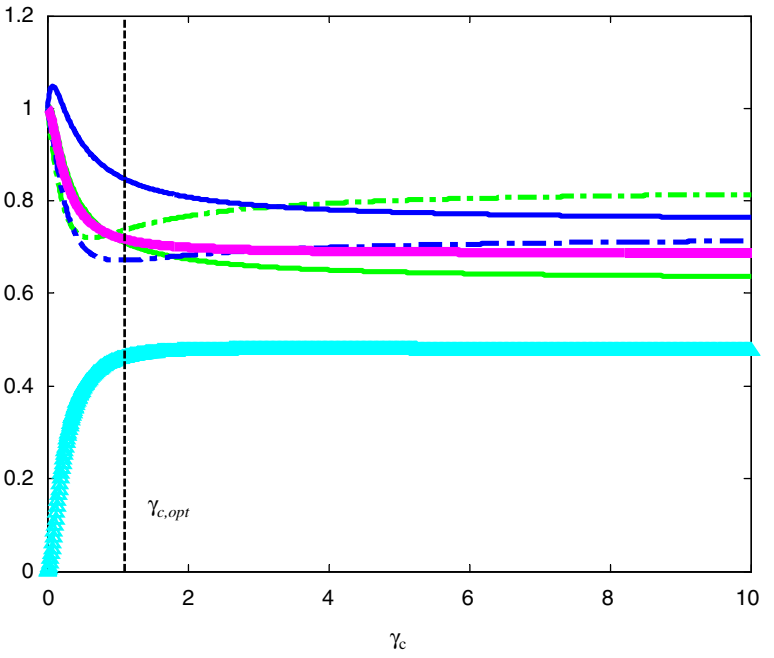

Fig. 10. WN and EPD: EDI index and response quantities versus γ_c, $\mu = 1$, $\lambda = 2$, and $\eta_{y,\mathrm{opt}} = 1.5$. Y_1, Y_2, A_1, A_2, ΔY, EDI.

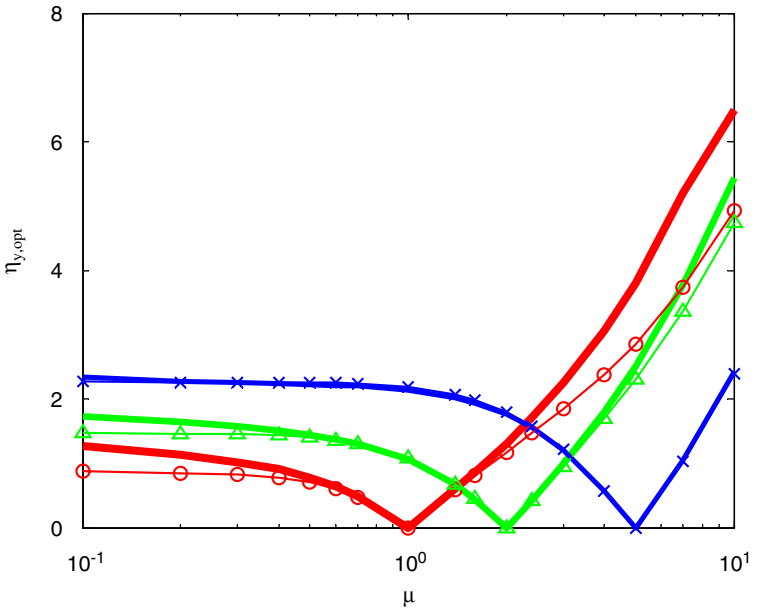

Fig. 11. WN: Comparison between optimal design spectrum of RPD and EPD ($\gamma_c = 1$). RPD: $\lambda = 1$, $\lambda = 2$, $\lambda = 5$. EPD: $\lambda = 1$, $\lambda = 2$, $\lambda = 5$.

The methodology may be also applied even if a filtered white noise is applied. As an example, the FWN defined in Section 2.3 has been used. Since in this case the excitation depends on frequency (or equivalently on period), as shown in Fig. 4, a further parameter, the natural period of the first structure T_1, has been considered.

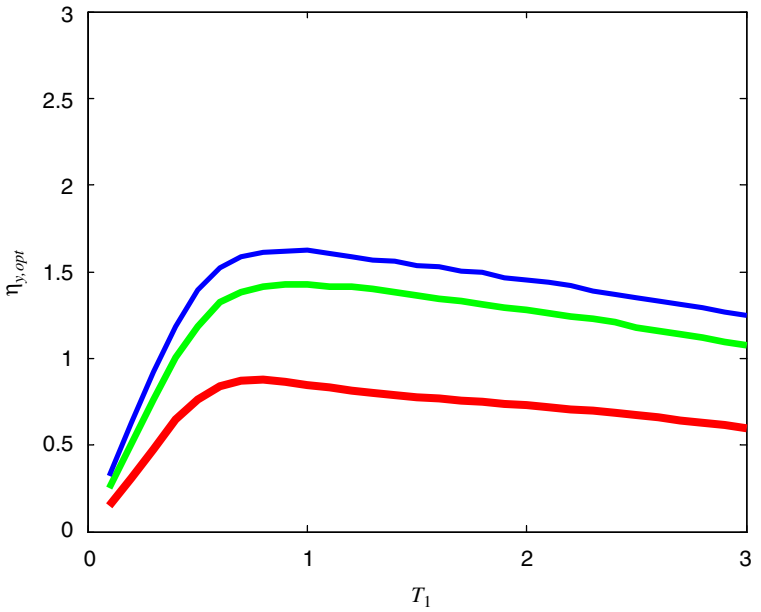

Fig. 12. FWN and EPD: optimal η_y versus T_1 for $\mu = 0.5$ and $\lambda = 1$, $\lambda = 2$, $\lambda = 5$.

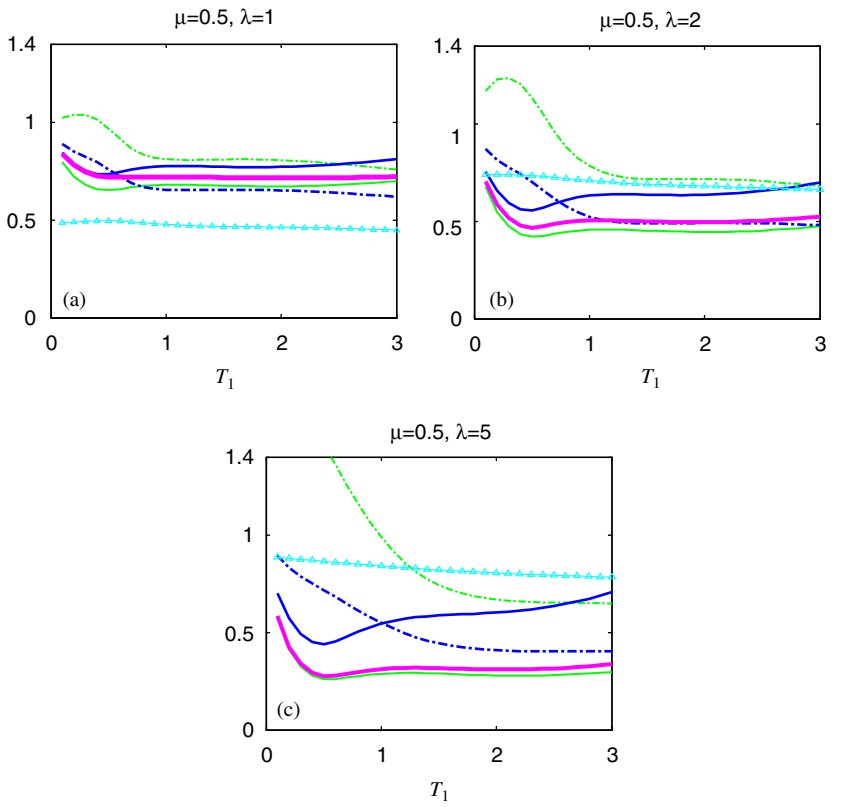

Fig. 13. FWN and EPD; response quantities versus T_1: (a) $\mu = 0.5$, $\lambda = 1$; (b) $\mu = 0.5$, $\lambda = 2$; (c) $\mu = 0.5$, $\lambda = 5$. Y_1, Y_2, A_1, A_2, ΔY, EDI.

It is important to remark that the two energy quantities, the mean value of ΔE_{dF} and EDI, are not equal, as previously discussed. In fact, in this case, the mean value of ΔE_i is not a constant value like in WN, Eq. (60). In this case, EDI index has been adopted as energy criterion.

In this context the optimal design of the connection has been carried out by performing a parametric analysis where the varying parameters are λ, μ, η_y and T_1.

Fig. 12 shows, for the EPD, some examples of optimal value of η_y versus T_1, for different values of λ (1, 2, 5) and $\mu = 0.5$. All response quantities and EDI versus T_1 for different values of λ (1, 2, 5) and $\mu = 0.5$ are presented in Fig. 13. In all cases, the period T_1 is greater than the period T_2, implying that the first structure is more flexible than the second structure.

For given values of λ, μ and T_1 by maximizing EDI index versus η_y, each optimal force and the corresponding response quantities, are presented in Figs. 12 and 13.

It is observed that the optimal η_y parameter, depends on the period. Moreover, different values of η_y, depending on the stiffness ratio λ, are obtained, however each curve has a regular and similar shape versus T_1. Spectra as the one depicted in Fig. 12, can be used to design the optimal hysteretic device; in this case the variables which need to be used are λ, μ and T_1. For the structural parameters λ and μ used in this particular study, the optimal η_y is obtained from the graph by selecting the value corresponding to the natural period of the first structure T_1. By looking at Fig. 13, it is important to notice how, in all the examples, EDI index appears almost constant versus the period T_1. Moreover, the EDI index appears to increase when the difference between λ and μ increases. In fact the greatest value for EDI is obtained when $\lambda = 5$, which corresponds to the maximum value of relative stiffness, Fig. 13c. In this situation, the two structures have very different dynamic characteristics and a large reduction of the seismic response of the flexible structure, with respect to the case with no connection, is observed. As for the optimal hysteretic device, the curves of Fig. 13 can be used to obtain the response reduction of the controlled system. In fact, by selecting the proper structural parameters μ and λ, the reduction of each response quantity is obtained by selecting the values corresponding to the period of the first structure T_1.

Having considered a wide range of variation of the parameters λ and μ (here not reported), the results lead to the conclusion that, as the stiffness ratio λ is large and the mass ratio μ is small, the connection works at its best in protecting the flexible structure, whereas the stiff structure is sacrificed (an amplification response is observed). Instead when the quantities μ and λ tend to have similar values, a reduction of all the responses for both structures is obtained.

6. Conclusions

An optimal methodology for the design of hysteretic dampers used as connection for two single dof systems has been proposed. For the hysteretic dampers the Bouc–Wen model has been adopted and a simplified solution of the nonlinear problem has been carried out using a stochastic linearization technique. To select the optimal hysteretic devices, an energy performance index, named EDI, has been introduced. This index is defined as the ratio of the maximum value of the energy dissipated in the devices, to the corresponding maximum value of the input energy.

At first a simple rigid plastic device, RPD, behavior is considered and the seismic excitation is modelled as a Gaussian zero mean white noise stochastic process.

In this case, the main results can be summarized as follows: (i) very simple curves are obtained for the optimal design of the hysteretic devices; (ii) the effectiveness of the RPD is evaluated by looking at the important response quantities as functions of the structural parameters; (iii) finally, some typical control applications have been discussed as a function of the control strategy, global and selective protection, and design parameters.

The optimal design methodology has been applied to solve practical problems by using more realistic modelling, for both the device and the seismic input.

With respect to the device, the difficulty to realize in the reality an RPD conducts to carry out an EPD characterized by the two parameters η_y and γ_c. It has been demonstrated that the relative stiffness γ_c can be chosen equal to one. The optimal design of the EPD with $\gamma_c = 1$ is carried out in comparison to the optimal design of the RPD. Considering the filtered white noise input, the same procedure leads to optimal design of

the connection, now depending also on the period of the first structure T_1. Considerations about the behavior of response quantities versus T_1 are finally made.

It is important to remark that the proposed methodology refers to a typical situation in civil engineering. However, in general, the procedure can simply be applied to solve any problem in other engineering fields, which refers to two structures, or two parts of the same structure, excited by an input that can be represented by a probabilistic approach.

References

[1] G.W. Housner, L.A. Bergman, T.K. Caughey, A.G. Chassiakos, R.O. Claus, S.F. Masri, R.E. Skelton, T.T. Soong, B.F. Spencer, J.T.P. Jao, Structural control: past, present and future, *Journal of Engineering Mechanics* 123 (9) (1997) 897–971.

[2] V. Ciampi, M. De Angelis, Optimal design of passive control systems based on energy dissipation for earthquake protection of structures, *Proceedings of the Third European Conference on Structural Dynamics*, EURODYN '96, Firenze, Italia, 1996, pp. 525–532.

[3] M. De Angelis, V. Ciampi, Effectiveness of dissipative connections on improving the earthquake response of adjacent structures, in: Duma (Ed.), *Tenth European Conference on Earthquake Engineering*, Balkema, Rotterdam, 1994, pp. 1891–1986.

[4] V. Ciampi, M. De Angelis, E. Renzi, *Optimal Design Selection of Special Connections Between Adjacent Structures in Passive and Semi-active Vibration Control Strategies*, *Proceedings of the Fourth European Conference on Structural Dynamics*, EURODYN '99, Balkema, Rotterdam, 1999, pp. 611–616.

[5] R.E. Christenson, B.F. Spencer JR, E.A. Johnson, Coupled building control using active and smart damping strategies, in: B.H.V. Topping, B. Kumar (Eds.), *Optimization and Control in Civil and Structural Engineering*, Civil-Comp Press, 1999, pp. 187–195.

[6] J.E. Luco, F.C.P. De Barros, Control of the seismic response of a composite tall building modelled by two interconnected shear beams, *Earthquake Engineering and Structural Dynamics* 27 (1998) 205–223.

[7] T. Kobori, T. Yamada, Y. Takenaka, Effect of dynamic tuned connector on reduction of seismic response—application to adjacent office buildings, *Proceedings of the Ninth World Conference Earthquake Engineering*, Vol. 5, Tokio-Kioto, Japan, 1988, pp. 773–778.

[8] T. Kobori, Y. Miura, E. Fukuzawa, T. Yamada, T. Arida, Y. Takenaka, N. Miyagawa, N. Tanaka, T. Fukumoto, Development and application of hysteresis steel dampers, *Proceedings of the Tenth World Conference Earthquake Engineering*, Vol. 4, Madrid, Spain, 1992, pp. 2341–2346.

[9] T. Sakurai, K. Shibata, S. Watanabe, A. Endoch, K. Yamada, Application of joint damper to thermal power plant buildings, *Proceedings of the Tenth World Conference Earthquake Engineering*, Vol. 7, Madrid, Spain, 1992, pp. 4149–4154.

[10] S. Soda, I. Kondo, S. Watabe, Experimental and analytical study on a structural design method to reduce seismic effects on a dual system, *Proceedings of the Ninth World Conference Earthquake Engineering*, Vol. 5, Tokio-Kioto, Japan, 1988, pp. 515–520.

[11] H.P. Hong, S.S. Wang, P. Hong, Critical building separation distance in reducing pounding risk under earthquake excitation, *Structural Safety* 25 (3) (2003) 287–303.

[12] R.H. Zhang, T.T. Soong, Seismic design of viscoelastic dampers for structural application, *Journal of Structural Engineering ASCE* 118 (5) (1992) 1375–1392.

[13] N. Makris, G.F. Dargush, M.C. Constantinou, Dynamic analysis of generalized viscoelastic fluids, *Journal of Engineering Mechanics ASCE* 119 (1993) 1663–1679.

[14] R.I. Skinner, R.G. Tyler, A.J. Heine, W.H. Robinson, Hysteretic dampers for the protection of structures from earthquakes, *Bulletin of New Zealand National Society for Earthquake Engineering* 13 (1) (1980) 22–36.

[15] J.M. Kelly, Base isolation in Japan, 1988. Report # UCB/EERC-88/20, University of California Berkeley, 1988.

[16] R.G. Tyler, Tapered steel energy dissipators for earthquake resistant structures, *Bulletin of New Zealand National Society for Earthquake Engineering* 11 (4) (1978) 282–294.

[17] A.S. Pall, C. March, Response of friction damped braced frames, *Journal of Structural Engineering ASCE* 108 (60) (1982) 1213–1323.

[18] A.S. Pall, V. Verganelakis, C. March, Friction dampers for seismic control of Concordia University library building, *Proceedings of the Fifth Canadian Conference On Earthquake Engineering*, Ottawa, Canada, 1987, pp. 191–200.

[19] H. Zhu, Y. Wen, H. Iemura, A study on interaction control for seismic response of parallel structures, *Computers & Structures* 7 (2001) 231–242.

[20] M. Kageyama, O. Yoshida, Y. Yasui, A study on optimum damping systems for connected double frame structures, *First World Conference on Structural Control*, Vol. 1, Los Angeles, CA, USA, 3–5 August 1994, IASC, session WP4, pp. 32–39.

[21] T. Aida, T. Aso, K. Takeshita, T. Takiuchi, T. Fujii, Improvement of the structure damping performance by interconnection, *Journal of Sound and Vibration* 242 (2) (2001) 333–353.

[22] W.S. Zhang, Y.K. Xu, Vibration analysis of two buildings linked by Maxwell model-defined fluid dampers, *Journal of Sound and Vibration* 233 (5) (2000) 775–796.

[23] Y.Q. Ni, J.M. Ko, Z.G. Ying, Random seismic response analysis of adjacent buildings coupled with non-linear hysteretic dampers, *Journal of Sound and Vibration* 246 (2001) 403–417.

[24] Y.Q. Ni, J.M. Ko, Z.G. Ying, Non-linear stochastic optimal control for coupled-structures system of multi-degree-of-freedom, *Journal of Sound and Vibration* 274 (2004) 843–861.

[25] Y.K. Wen, Equivalent linearization for hysteretic systems under random excitation, *American Society of Mechanical Engineers Journal of Applied Mechanics* 47 (1980) 150–154.

[26] Y.K. Wen, Method for random vibration of hysteretic systems, *Journal of the Engineering Mechanics Division, Proceedings of the American Society of Civil Engineers* 102 (1976) 249–263.
[27] K. Kanai, *Seismic-empirical formula for the seismic characteristics of the ground*, Vol. 35, Bulletin of the Earthquake Research Institute, University of Tokio, pp. 309–325.
[28] H. Tajimi, A statistics method of determining the maximum response of a building structure during an earthquake, *Proceedings of the Second World Conference on Earthquake Engineering*, 1960, pp. 781–798.
[29] R.W. Clough, J. Penzien, *Dymamics of Structures*, McGraw-Hill, New York, 1995.
[30] T.T. Soong, M. Grigoriu, *Random Vibration of Mechanical and Structural Systems*, Prentice-Hall, Englewood Cliffs, NJ, 1993.
[31] Y.K. Lin, *Probabilistic Theory of Structural Dynamics*, McGraw-Hill, New York, 1967.
[32] C.M. Uang, V.V. Bertero, Use of energy as design criterion in earthquake-resistant design, Report No. UCB/EERC-88/18, November 1998, Earthquake Engineering Research Center, University of California, Berkeley.
[33] J.A. Inaudi, A. Zambrano, J. Kelly, On the analysis of structures with viscoelastic dampers, 1993, UBC/EERC Report No. 93/06.